

Comparison of Modulator Retention Shapes for Radial Flux Coaxial Magnetic Gears

Salek A. Khan

Dept. of Electrical & Computer Engineering
University of Texas at Dallas
Richardson, Texas, United States
salek@utdallas.edu

Godwin Duan

Dept. of Electrical & Computer Engineering
Princeton University
Princeton, New Jersey, United States
gd9138@princeton.edu

Matthew C. Gardner

Dept. of Electrical & Computer Engineering
University of Texas at Dallas
Richardson, Texas, United States
matthew.gardner@utdallas.edu

Abstract— Magnetic gears perform the same function as mechanical gears using magnetic fields instead of interlocking teeth. The radial flux coaxial magnetic gear, the most common topology, requires a set of magnetically permeable modulators, which must be supported against strong magnetic forces. A bridge is often employed to connect the modulators together, but this reduces the slip torque. This paper proposes a new crescent-shaped feature, which allows modulators to be supported solely by nonmagnetic material between the modulators without a bridge. Using 2D finite element analysis, its slip torque performance is compared to bridged modulator designs and two other curved, bridgeless modulator designs. For lower modulator counts, a modulator with curved indents on both sides can slightly increase the slip torque. However, for higher modulator counts, the proposed crescent-shaped modulator outperforms other modulator retention strategies.

Keywords— modulator retention, finite-element analysis (FEA), magnetic gear, pole piece shape, torque density, torque ripple, efficiency

I. INTRODUCTION

Magnetic gears transfer power between high-speed, low-torque rotation and low-speed, high-torque rotation using modulated magnetic fields. Their contactless gearing action makes them attractive for a wide variety of applications, such as hydrokinetic [1], [2] and wind [3], [4] energy generation, aerospace applications [5], [6], and vehicles [7], [8]. Much of the research on magnetic gears has focused on the radial flux coaxial magnetic gear [1]-[13] illustrated in Fig. 1. It consists of two permanent magnet (PM) rotors and a set of magnetically permeable modulators between them. The modulator count (Q_2) and number of PM pole pairs on the inner rotor (P_1) and the outer rotor (P_3) are related by

$$Q_2 = P_1 + P_3. \quad (1)$$

The modulators must be supported against the strong pull of the PMs. Often, a thin bridge connects the modulators together in a ring to simplify fabrication and increase stiffness, as shown in Fig. 2(a), but this provides a path for flux leakage, which reduces the slip torque [1]-[3], [7], [8], [11], [13]. However, bridges are not universally employed [5], [14]. With or without a bridge, nonmagnetic material is placed between the modulators to support the forces and torques applied on the modulators [1], [5], [7], [8], [11], [13], [14]. Some previous studies have evaluated the impacts of modulator shapes [8], [15], but these studies have evaluated a fairly limited range of shapes.

Other studies have evaluated different bridges [1], [8], [11], [12], [16]-[18]. These studies have generally concluded that torque is maximized by keeping the bridge thin and near the high-pole-count rotor (Rotor 1). Some studies have also indicated that the bridge can reduce eddy current losses in the PMs [1], [11].

To facilitate the transfer of radial forces between the modulators and the support material, protruding or indented features should be added to the modulators to allow them to interlock with the support material, particularly for designs without a bridge. For example, [5] uses modulators with curved indents on both sides, similar to Fig. 2(b). Alternatively, the

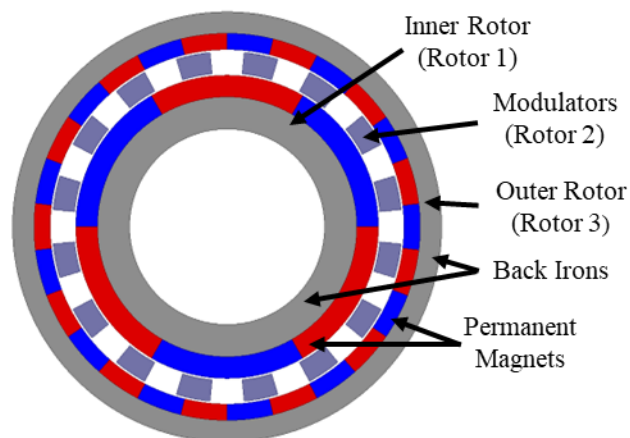


Fig. 1. Cross-section of a radial flux coaxial magnetic gear.

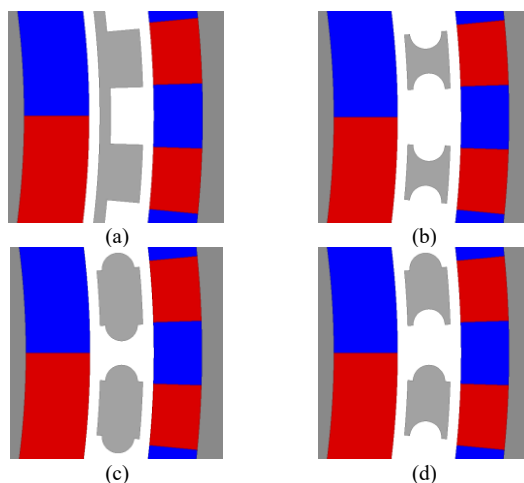


Fig. 2. (a) Bridge-connected modulator. (b) Both sides protruding. (c) Both sides indented. (d) Proposed crescent-shaped feature.

modulators could have protrusions, as in Fig. 2(c) or [14]. We propose crescent-shaped modulators, shown in Fig. 2(d). Each modulator has a curved indent on one side and a curved protrusion on the other side. This allows magnetic flux to pass through with less constriction or saturation than Fig. 2(b) and with less flux leakage between modulators than Fig. 2(c). Thus, we expect that the crescent-shaped modulators may offer higher slip torques than the other three options. The performances of these four modulators types are compared using 2D finite element analysis (FEA).

II. DESIGN STUDY

A 2D parametric FEA sweep was performed to investigate the effects of different modulator shapes. Designs with curved modulators, shown in Figs. 2(b)-(d), were compared to designs with straight-edged, bridge-connected modulators (Fig. 2(a)). Various cases for each shape were simulated with different parameters, which are listed in Tables I and II and illustrated in Fig. 3. The back irons and modulators were M19 electrical steel, and the PMs were N50H grade NdFeB. Cases with $L_{Curve} < 2D_{Curve}$ were excluded. α_{In} and α_{Out} are defined in

$$\alpha_{In} = \frac{\theta_{In,1}}{\theta_{In,2}} \quad (2)$$

$$\alpha_{Out} = \frac{\theta_{Out,1}}{\theta_{Out,2}} \quad (3)$$

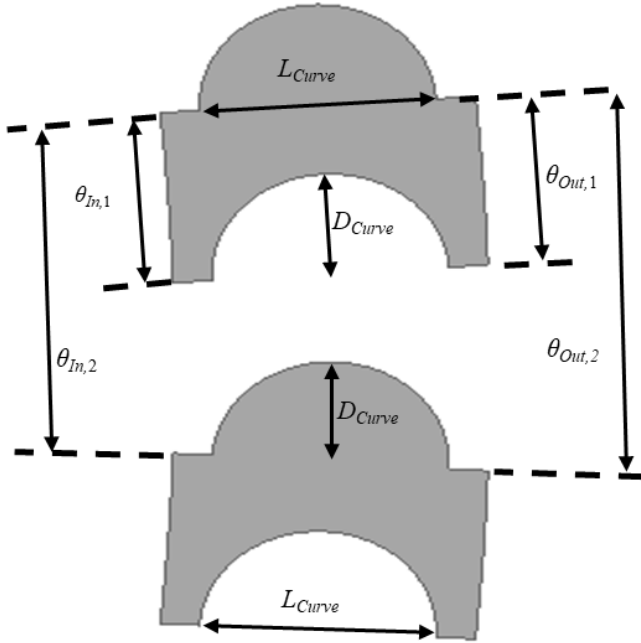


Fig. 3. Modulator sweep parameters.

TABLE I. BASE DESIGN PARAMETERS

Symbol	Description	Value
R_{Out}	Outer radius	100 mm
T_{BI}	Back iron thicknesses	5 mm
T_{PM1}	Rotor 1 magnet thickness	6 mm
T_{PM3}	Rotor 3 magnet thickness	4.5 mm
T_{AG}	Airgaps	1 mm
T_{Mods}	Modulator thickness	8 mm
α_{PM}	Magnet fill factor	1

TABLE II. SWEEP MODULATOR PARAMETERS

Symbol	Description	Values
α_{In}	Modulator inner tangential fill factor	0.05,0.1,...0.95
α_{Out}	Modulator outer tangential fill factor	0.05,0.1,...0.95
D_{Curve}	Modulator curvature tangential depth	1,2,3 mm
L_{Curve}	Modulator curvature radial length	2,4,6 mm
T_{Bridge}	Modulator bridge thickness	0.5,1,1.5 mm

III. DATA TRENDS

A. All Modulator Parameters

First, a design with a relatively low number of modulators ($P_1 = 3, Q_2 = 26, P_3 = 23$) was evaluated. Fig. 4 shows the torque densities achievable using the different modulator retention strategies for different bridge thicknesses or curvature depths. Fig. 5 shows the modulators of the optimal designs in Fig. 4, with the circled numbers identifying which design corresponds to which point in Fig. 4. In this low modulator count case, the indented shape (Fig. 2(b)) offers the largest slip torque. Interestingly, it is even slightly better than the shape with no retention features. This may be because the modulators are relatively large in this low modulator count case, so adding indents can reduce flux leakage between modulators without saturating the modulators. The two-sided protruding design (Fig. 2(c)) and the proposed crescent design (Fig. 2(d)) offer lower slip torques than the indented shape. Since the modulators are already large, the protrusions in these two shapes likely do not help to channel more flux; instead, they increase flux leakage to neighboring modulators. Nevertheless, all three curved shapes at a 3 mm curvature depth have a higher slip torque than the 1 mm and 1.5 mm bridge designs.

Additionally, the effects of the different retention strategies on both torque ripple (peak-to-peak divided by average) and electromagnetic (EM) efficiency were analyzed, and the results are shown in Figs. 6-8.

Without any features, the Rotor 1 torque ripple is significant, but the Rotor 2 torque ripple is a much smaller percentage of the average torque. Overall, the bridge did significantly reduce the torque ripple on both rotor 1 and 2. Similarly, all retention strategies reduced the torque ripple as the curvature depth increased. Fig. 8(a) shows that very thin bridges actually improve the efficiency slightly as compared to no bridge or a thicker bridge. This is consistent with the

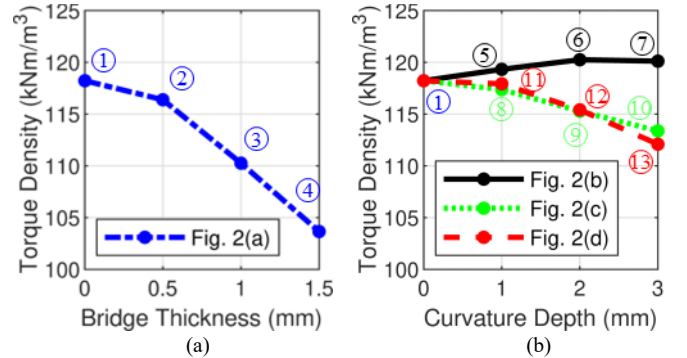


Fig. 4. Effects of (a) bridge thickness or (b) the curvature depth of the interlocking features on the achievable torque density for the low modulator count design.

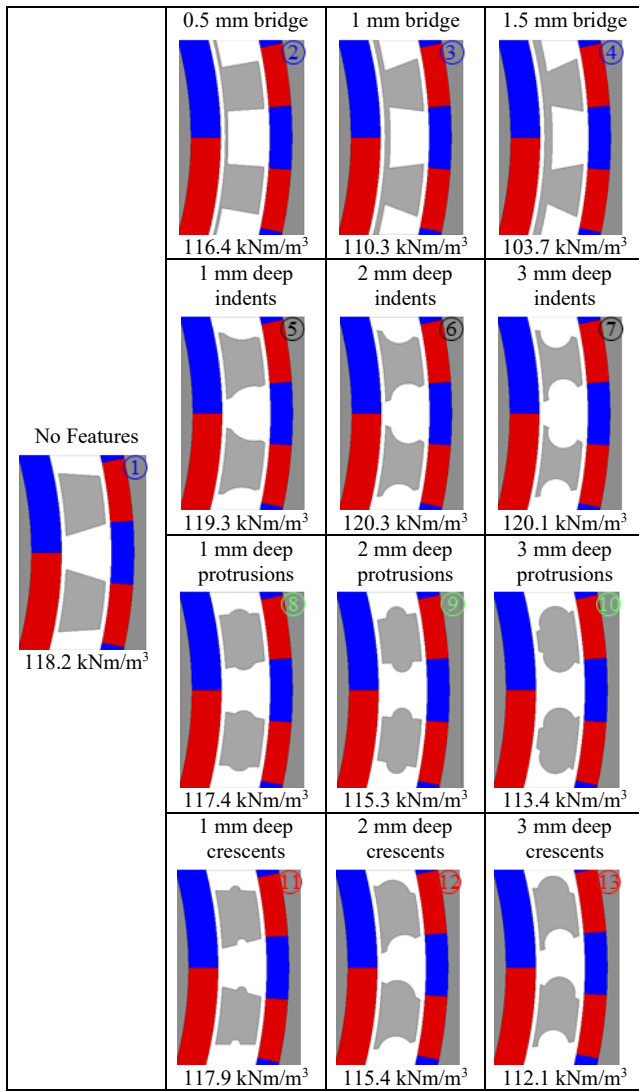


Fig. 5. Optimal low count modulator designs

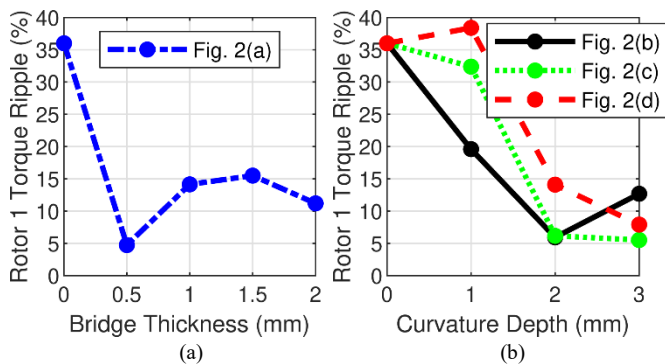


Fig. 6. Effects of (a) bridge thickness or (b) the curvature depth of the interlocking features on the Rotor 1 torque ripple for the designs depicted in Fig. 5.

reduction in PM eddy current losses resulting from the bridge in [1], [11]. Similarly, Fig. 8(b) shows that the interlocking features can also provide a slight increase in efficiency. Both the bridge and the interlocking features tend to smooth out the sharp edges of the air gap permeance function (when saturation

is considered); this may reduce the magnitude of some of the high order harmonics in the magnetic flux density, which would reduce losses. However, the torque ripple and efficiency trends are generally not monotonic. A possible explanation for this is, because all the variables from Table II are being swept at once, it is difficult to analyze how each individual parameter affects the torque ripple. To get a better idea of how each retention strategy affects the torque ripple, simulations were run where the only parameter that was changed was which feature (bridges, indents, protrusions, or crescents) was being used. The results of these designs are discussed in depth in the next subsection.

Next, a design with a higher number of modulators ($P_1 = 7$, $Q_2 = 86$, $P_3 = 79$) was considered. Fig. 9 compares the achievable torque densities with the different modulator features. Fig. 10 shows the modulators of the optimal designs in Fig. 9. Because the higher modulator count results in much tangentially narrower modulators, the 3 mm curvature depth for the cases with two indents (Fig. 2(b)) or two protrusions (Fig. 2(c)) are infeasible. Here, the proposed crescent-shaped modulator design (Fig. 2(d)), which maintains a roughly constant modulator width, is superior to the indented model (Fig. 2(b)), which suffers from saturation in the middle of the modulators, and the protruding model (Fig. 2(c)), which suffers from increased flux leakage between modulators. For a 2 mm curvature depth, the proposed crescent-shaped design has higher slip torque than a design with a 1 mm or 1.5 mm bridge. However, the torque falls rapidly as the curvature depth increases to 3 mm, due to increased flux leakage.

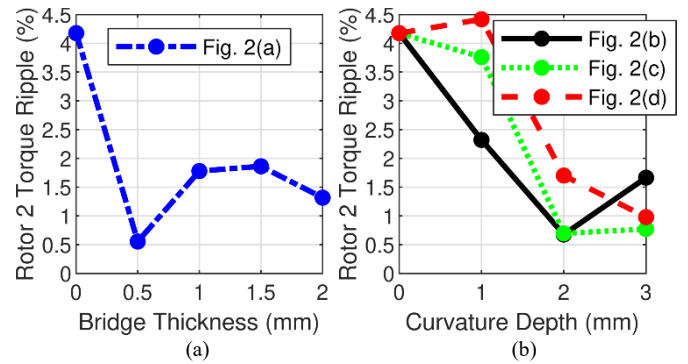


Fig. 7. Effects of (a) bridge thickness or (b) the curvature depth of the interlocking features on the Rotor 2 torque ripple for the designs depicted in Fig. 5.

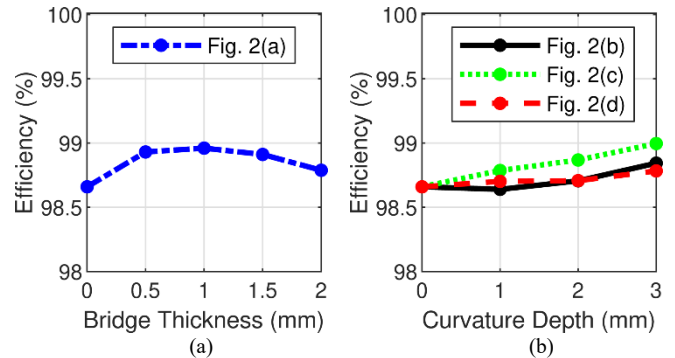


Fig. 8. Effects of (a) bridge thickness or (b) the curvature depth of the interlocking features on the EM efficiency for the designs depicted in Fig. 5.

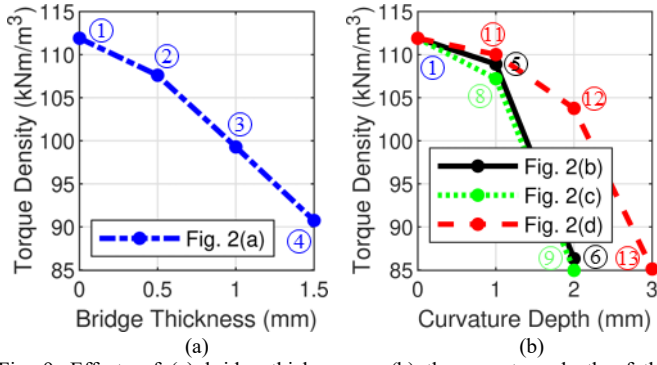


Fig. 9. Effects of (a) bridge thickness or (b) the curvature depth of the interlocking features on the achievable torque density for the high modulator count design.

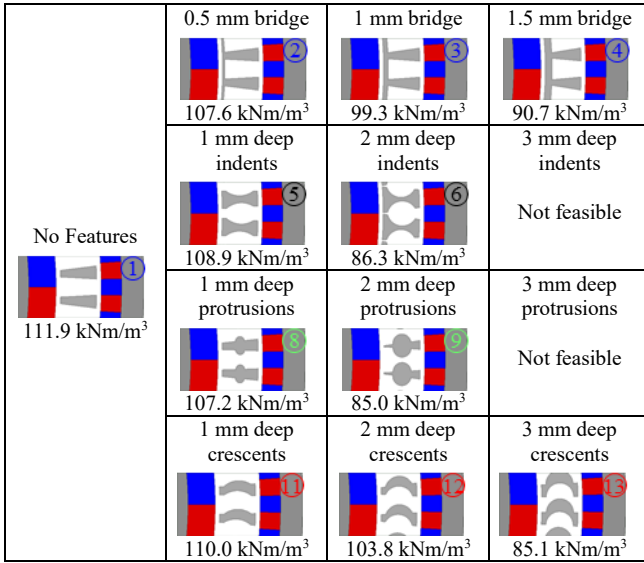


Fig. 10. Optimal high count modulator designs

Figs. 11 and 12 show that this design has much lower torque ripple on both Rotor 1 and Rotor 2 than the design with fewer poles and modulators. (This is due to the lower ripple factor [19].) Thus, the impacts of the bridge and retention features on torque ripple tend to be less significant than for the design with fewer poles and modulators.

Fig. 13(a) shows that the efficiency decreases as the bridge thickness increases. This is because as the bridge gets thicker, more flux is shorted in the bridge itself, which reduces the torque while increasing core losses in the bridge itself. For this design, these factors outweigh the reduction in PM losses. Fig. 13(b) appears to show that the protrusions actually increase the efficiency slightly. However, this may be the result of α_{In} and α_{Out} varying between cases.

B. Isolated Retention Features Analysis

Fig. 14 shows the torque density for the designs where only the retention features were analyzed. For these cases, α_{In} and α_{Out} were each fixed at 0.5, and L_{Curve} was set to 6 mm. Fig. 15 shows these designs. The trends in torque density versus curvature depth, were more or less the same as when all the modulator parameters were swept, except the indented designs.

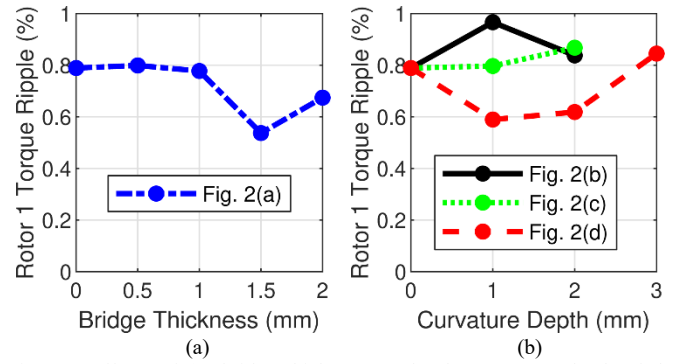


Fig. 11. Effects of (a) bridge thickness or (b) the curvature depth of the interlocking features on the Rotor 1 torque ripple for the designs depicted in Fig. 10.

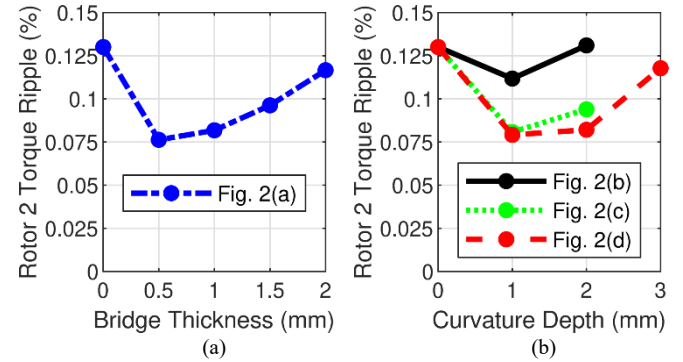


Fig. 12. Effects of (a) bridge thickness or (b) the curvature depth of the interlocking features on the Rotor 2 torque ripple for the designs depicted in Fig. 10.

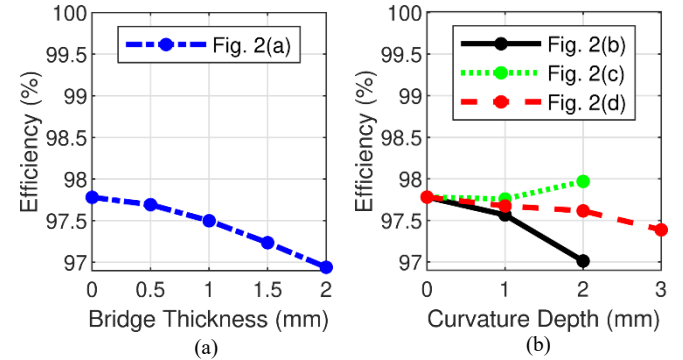


Fig. 13. Effects of (a) bridge thickness or (b) the curvature depth of the interlocking features on the EM efficiency for the designs depicted in Fig. 10.

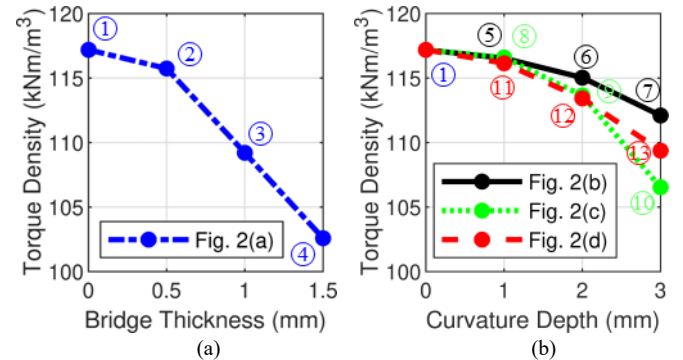


Fig. 14. Effects of (a) bridge thickness or (b) the curvature depth of the interlocking features on the torque density for the low modulator count design where the retention features were isolated.

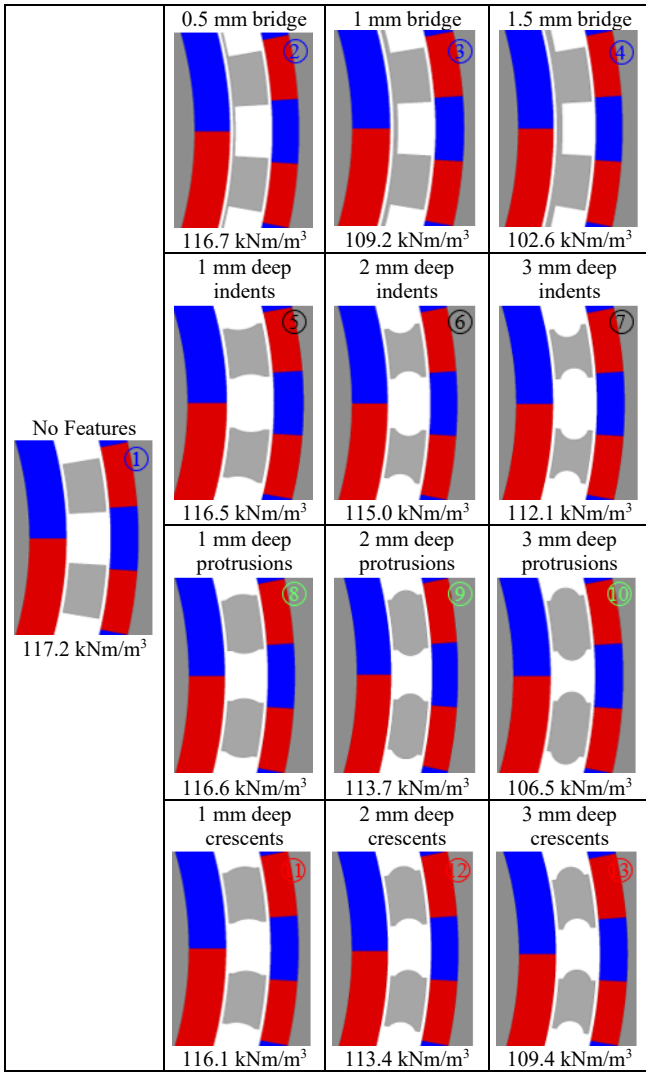


Fig. 15. Low modulator count designs with isolated retention features parameters

Interestingly, when all the modulator parameter values were swept (Fig. 4(b)), the curvature depth for the indented cases had a much weaker effect on the torque density. In these designs, increasing the indent curvature depth seems to impact the torque density to a greater extent because the other parameters could not compensate for the indents or bulges.

Fig. 16 and Fig. 17 show the effects of bridge thickness or curvature depth on the Rotor 1 and Rotor 2 torque ripple, respectively. Fig. 18 shows how the EM efficiency is affected by bridge thickness or curvature depth. Figs. 16(a) and 17(a) show that increasing the bridge thickness significantly reduces the torque ripple. Figs. 16(b) and 17(b) show that all retention strategies actually reduce the torque ripple as the curvature depth increases. In Fig. 18(a), a small bridge thickness of 0.5 mm provides a small gain in efficiency by reducing eddy current losses in the Rotor 1 PMs. Fig. 18(b) shows that the other retention strategies do not significantly change the EM efficiency, with the protruded design seeing a very slight benefit with larger curvature depths. Each of these torque ripple

or efficiency benefits likely occurs because the bridge or retention features smooth out the sharp edges in the air gap permeance function.

Fig. 19 illustrates the impacts of the various retention features on the torque density of the high modulator count design, and Fig. 20 shows the modulator shapes of these designs. (For the high modulator count case with $\alpha_{In} = \alpha_{Out} = 0.5$, 2 mm, designs with 2 mm indents or bulges on each side were infeasible, so designs with 1.5 mm indents or bulges were evaluated instead.) As with the previous case, the retention features have a more detrimental impact on torque density when the other modulator parameters are fixed. Figs. 21 and 22 show the effects of retention features on torque ripple.

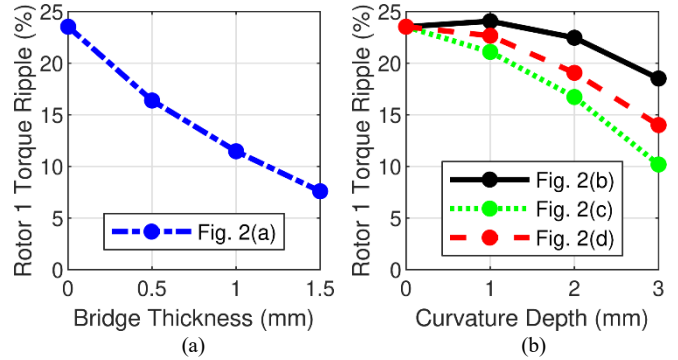


Fig. 16. Effects of (a) bridge thickness or (b) the curvature depth of the interlocking features on the Rotor 1 torque ripple for the low modulator count design where the retention features were isolated.

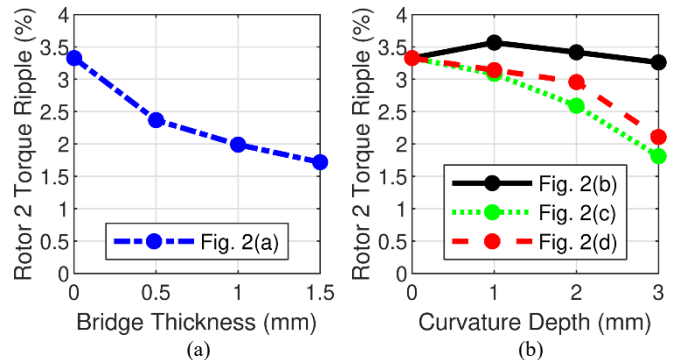


Fig. 17. Effects of (a) bridge thickness or (b) the curvature depth of the interlocking features on the Rotor 2 torque ripple for the low modulator count design where the retention features were isolated.

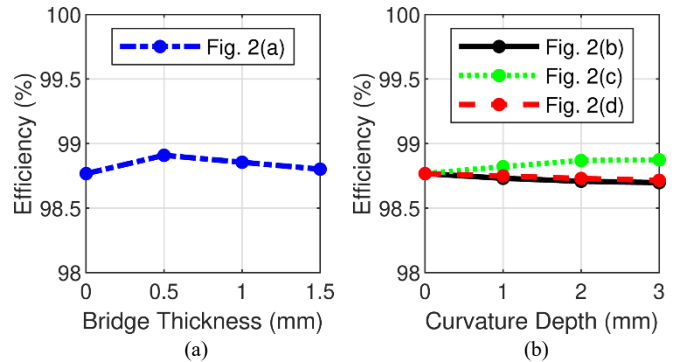


Fig. 18. Effects of (a) bridge thickness or (b) the curvature depth of the interlocking features on the EM efficiency for the low modulator count design where the retention features were isolated.

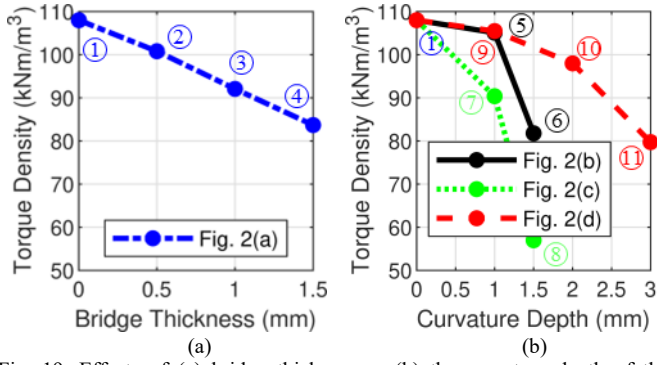


Fig. 19. Effects of (a) bridge thickness or (b) the curvature depth of the interlocking features on the torque density for the high modulator count design where the retention features were isolated.

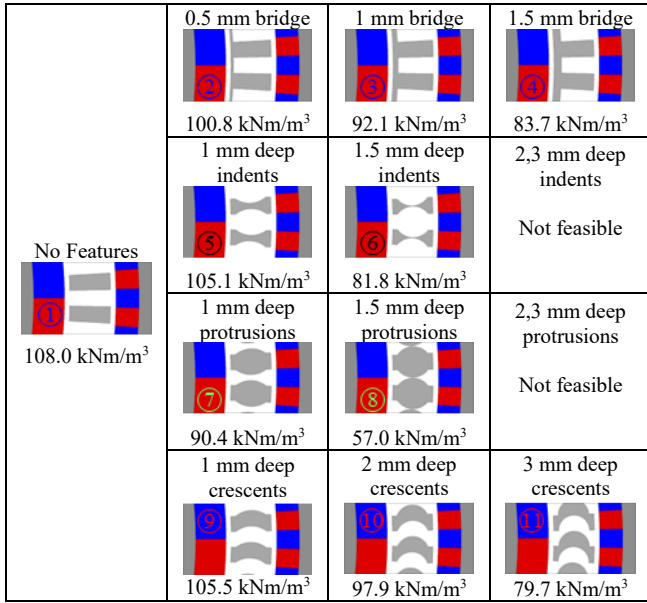


Fig. 20. High modulator count designs with isolated retention features parameters

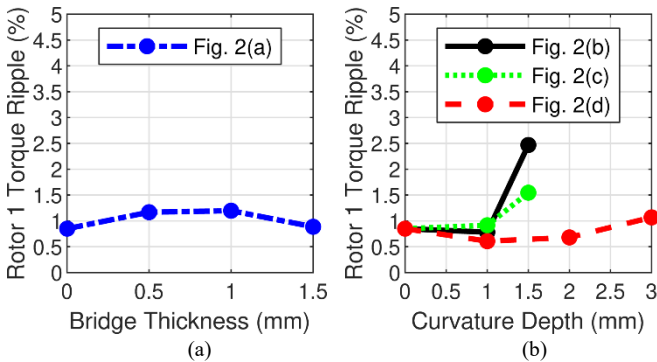


Fig. 21. Effects of (a) bridge thickness or (b) the curvature depth of the interlocking features on the Rotor 1 torque ripple for the high modulator count design where the retention features were isolated.

When the retention feature significantly reduces the average torque (see Fig. 19), the torque ripple percentage can increase significantly. Fig. 23 illustrates that the retention features tend to decrease efficiency, which is likely due to the reduction in average torque.

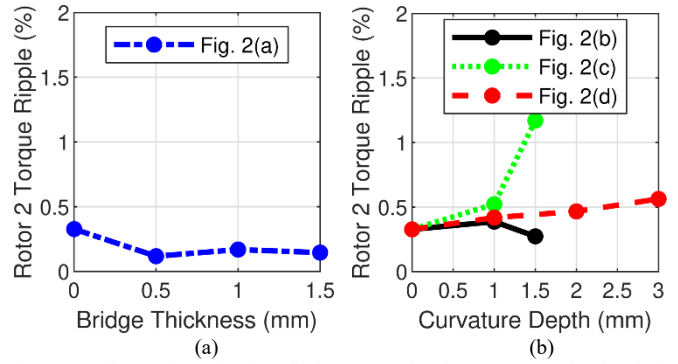


Fig. 22. Effects of (a) bridge thickness or (b) the curvature depth of the interlocking features on the Rotor 2 torque ripple for the high modulator count design where the retention features were isolated.

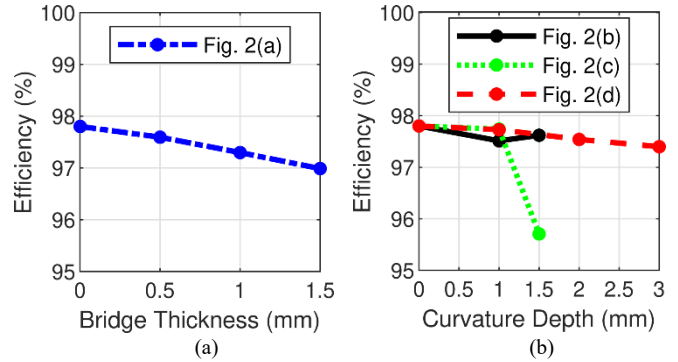


Fig. 23. Effects of (a) bridge thickness or (b) the curvature depth of the interlocking features on the EM efficiency for the high modulator count design where the retention features were isolated.

IV. CONCLUSION

This paper introduces a crescent shaped modulator that aims to provide an effective modulator retention strategy while not requiring a bridge. This new design is compared against the conventional bridge, as well as both protruding and indented modulator shapes. Since the number of modulators is dependent on the pole count, both a low and high pole count design were considered. To better understand the independent effect of the modulator shape, designs with all parameters fixed except the support type were evaluated. Lastly, the effect of the modulator retention strategies on both torque ripple and efficiency was analyzed. Based on the FEA simulation studies, the following conclusions can be drawn:

- For low modulator counts, indents on both sides of a modulator can increase the slip torque.
- For high modulator counts, the proposed crescent shape retains its slip torque best, especially for higher curvature depths.
- Modulators with a significant amount of curvature can achieve higher torques than designs with all but the thinnest of bridges.
- For both high and low modulator counts, the bridged designs significantly reduced torque ripple on both Rotor 1 and Rotor 2.
- The other retaining features could also reduce the torque ripples, but their impacts were not as significant as that of the bridge.

- For low modulator counts, the modulator retention strategy did not significantly affect the EM efficiency, but it could increase the EM efficiency very slightly for some cases.
- For high modulator counts, the modulator retention feature tends to reduce EM efficiency as the feature tends to reduce average torque.

REFERENCES

- [1] M. Johnson, M. C. Gardner, H. A. Toliyat, S. Englebretson, W. Ouyang, and C. Tschida, "Design, Construction, and Analysis of a Large-Scale Inner Stator Radial Flux Magnetically Geared Generator for Wave Energy Conversion," *IEEE Trans. Ind. Appl.*, vol. 54, no. 4, pp. 3305-3314, Jul.-Aug. 2018.
- [2] H. Baninajar, S. Modaresahmadi, H. Y. Wong, J. Z. Bird, W. Williams, and B. Dechant, "Designing a Halbach Rotor Magnetic Gear for a Marine Hydrokinetic Generator," *IEEE Trans. Ind. Appl.*, 2022, early access.
- [3] K. Li, S. Modaresahmadi, W. B. Williams, J. D. Wright, D. Som, and J. Z. Bird, "Designing and experimentally testing a magnetic gearbox for a wind turbine demonstrator," *IEEE Trans. Ind. Appl.*, vol. 55, no. 4, pp. 3522-3533, Jul.-Aug. 2019.
- [4] L. Jian, K. T. Chau, and J. Z. Jiang, "A Magnetic-Geared Outer-Rotor Permanent-Magnet Brushless Machine for Wind Power Generation," *IEEE Trans. Ind. Appl.*, vol. 45, no. 3, pp. 954-962, May-Jun. 2009.
- [5] J. J. Scheidler, V. M. Asnani, and T. F. Tallerico, "NASA's magnetic gearing Research for Electrified Aircraft Propulsion," in *Proc. AIAA/IEEE Elect. Aircraft Technol. Symp.*, 2018, pp. 1-12.
- [6] R. S. Dragan, R. E. Clark, E. K. Hussain, K. Atallah, and M. Odavic, "Magnetically Geared Pseudo Direct Drive for Safety Critical Applications," *IEEE Trans. Ind. Appl.*, vol. 55, no. 2, pp. 1239-1249, Mar.-Apr. 2019.
- [7] T. V. Frandsen, P. O. Rasmussen, and K. K. Jensen, "Improved motor integrated permanent magnet gear for traction applications," in *Proc. IEEE Energy Convers. Congr. Expo*, 2012, pp. 3332-3339.
- [8] L. Jing, W. Tang, T. Wang, T. Ben, and R. Qu, "Performance Analysis of Magnetically Geared Permanent Magnet Brushless Motor for Hybrid Electric Vehicles," *IEEE Trans. Transport. Electrific.*, vol. 8, no. 2, pp. 2874-2883, Jun. 2022.
- [9] K. Atallah and D. Howe, "A novel high-performance magnetic gear," *IEEE Trans. Magn.*, vol. 37, no. 4, pp. 2844-2846, July 2001.
- [10] P. O. Rasmussen, T. O. Anderson, F. T. Jorgensen, and O. Nielsen, "Development of a high performance magnetic gear," *IEEE Trans. Ind. Appl.*, vol. 41, no. 3, pp. 764-770, May-Jun. 2005.
- [11] M. C. Gardner, M. Johnson, and H. A. Toliyat, "Performance Impacts of Practical Fabrication Tradeoffs for a Radial Flux Coaxial Magnetic Gear with Halbach Arrays and Air Cores," in *Proc. IEEE Energy Convers. Congr. Expo*, 2019, pp. 3129-3136.
- [12] S. J. Kim, E. Park, S. Jung, and Y. Kim, "Transfer Torque Performance Comparison in Coaxial Magnetic Gears With Different Flux-Modulator Shapes," *IEEE Trans. Magn.*, vol. 53, no. 6, pp. 1-4, Jun. 2017.
- [13] S. Gerber and R. Wang, "Evaluation of a prototype magnetic gear," in *Proc. IEEE Int. Conf. Ind. Technol.*, 2013, pp. 319-324.
- [14] M. Johnson, M. C. Gardner, and H. A. Toliyat, "Design and Analysis of an Axial Flux Magnetically Geared Generator," *IEEE Trans. Ind. Appl.*, vol. 53, no. 1, pp. 97-105, Jan.-Feb. 2017.
- [15] S. -J. Kim, C. -H. Kim, S. -Y. Jung, and Y. -J. Kim, "Optimal Design of Novel Pole Piece for Power Density Improvement of Magnetic Gear Using Polynomial Regression Analysis," *IEEE Trans. Energy Convers.*, vol. 30, no. 3, pp. 1171-1179, Sep. 2015.
- [16] D. Z. Abdelhamid and A. M. Knight, "The Effect of Modulating Ring Design on Magnetic Gear Torque," *IEEE Trans. Magn.*, vol. 53, no. 11, pp. 1-4, Nov. 2017.
- [17] L. Jian, Z. Deng, Y. Shi, J. Wei, and C. C. Chan, "The Mechanism How Coaxial Magnetic Gear Transmits Magnetic Torques Between Its Two Rotors: Detailed Analysis of Torque Distribution on Modulating Ring," *IEEE/ASME Trans. Mechatronics*, vol. 24, no. 2, pp. 763-773, Apr. 2019.
- [18] N. W. Frank and H. A. Toliyat, "Analysis of the Concentric Planetary Magnetic Gear With Strengthened Stator and Interior Permanent Magnet Inner Rotor," *IEEE Trans. Ind. Appl.*, vol. 47, no. 4, pp. 1652-1660, Jul.-Aug. 2011.
- [19] B. Praslicka, M. C. Gardner, M. Johnson, and H. A. Toliyat, "Review and Analysis of Coaxial Magnetic Gear Pole Pair Count Selection Effects," *IEEE Trans. Emerg. Sel. Topics Power Electron.*, vol. 10, no. 2, pp. 1813-1822, Apr. 2022..